Supporting Information

Zhang et al. 10.1073/pnas.1800234115

To address the possibility that polaron formation increases the volume of the system, as well as to examine the coupling of charge carriers to the organic crystal, we performed additional MD simulations, using the PIMD formalism to simulate an excess electron in DBTTF-C_{60} (1–3). In this approach, one exploits the isomorphism between the statistical mechanics of a quantum particle with that of a classical ring polymer, to simulate the electron as a classical ring polymer with P beads (4). Intrapolymer interactions consist only of nearest-neighbor harmonic bonds that account for the quantum nature of the particle. Interactions between the electron and DBTTF are given by Shaw-type pseudopotentials (5); the electron–C_{60} interactions are described by the pseudopotential of Mayer, which was developed for graphene and carbon nanotubes (6). This PIMD approach enables us to efficiently simulate a free charge carrier (electron) in the DBTTF-C_{60} lattice, and has previously been employed to describe polaron formation in many complex systems (1, 3, 7–9). PIMD simulations were performed in the canonical ensemble, and Fig. S6 shows a snapshot of the bulk structure with and without an excess electron. We find that the presence of an excess electron increases the pressure of the system with respect to the pure solid at fixed volume by ∼2 kbar. The increase in pressure indicates that accommodating an excess electron will lead to expansion of the system. This suggests that the coupling of photoexcited charge carriers to the DBTTF-C_{60} lattice can contribute to photostriction and its dependence on film thickness. We expect this qualitative result, increasing pressure to accommodate a free charge carrier, to be true for any reasonable choice of electron–lattice interaction potentials, but note that pseudopotentials parameterized specifically for this system may lead to more accurate estimates of the pressure increase.

1. Sprik M, Klein ML (1988) Application of path integral simulations to the study of electron solvation in polar fluids. *Comput Phys Rep* 7:147–166.
2. Habershon S, Manolopoulos DE, Markland TE, Miller TF, 3rd (2013) Ring-polymer molecular dynamics: Quantum effects in chemical dynamics from classical trajectories in an extended phase space. *Annu Rev Phys Chem* 64:387–413.
3. Berne BJ, Thirumalai D (1986) On the simulation of quantum systems: Path integral methods. *Annu Rev Phys Chem* 37:401–424.
4. Chandler D, Wolynes PG (1981) Exploiting the isomorphism between quantum theory and classical statistical mechanics of polyatomic fluids. *J Chem Phys* 74:4078–4095.
5. Shaw RW, Jr (1968) Optimum form of a modified Heine-Abarenkov model potential for the theory of simple metals. *Phys Rev* 174:769–781.
6. Mayer A (2004) Band structure and transport properties of carbon nanotubes using a local pseudopotential and a transfer-matrix technique. *Carbon* 42:2057–2066.
7. Deng Z, Martyna GJ, Klein ML (1994) Quantum simulation studies of metal–ammonia solutions. *J Chem Phys* 100:7590–7601.
8. Chandler D, Leung K (1994) Excess electrons in liquids: Geometrical perspectives. *Annu Rev Phys Chem* 45:557–591.
9. Bischak CG, et al. (2017) Origin of reversible photoinduced phase separation in hybrid perovskites. *Nano Lett* 17:1028–1033.

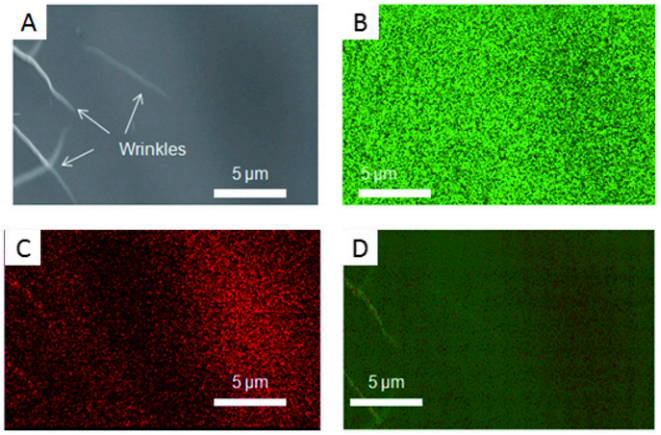

Fig. S1. SEM image (*A*) and elemental mapping images (*B–D*), with a uniform element distribution of carbon (*B*) and sulfur (*C*) elements, implying chemical uniformity. (*D*) Stacked mapping image of carbon and sulfur elements.

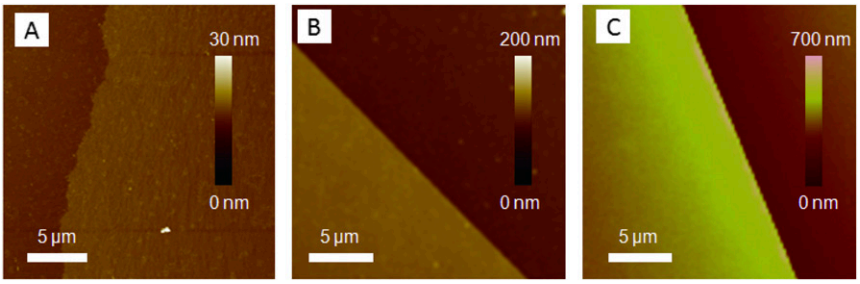

Fig. S2. AFM images of typical samples with average thickness of nearly 10 (*A*), 90, (*B*) and 300 nm (*C*).

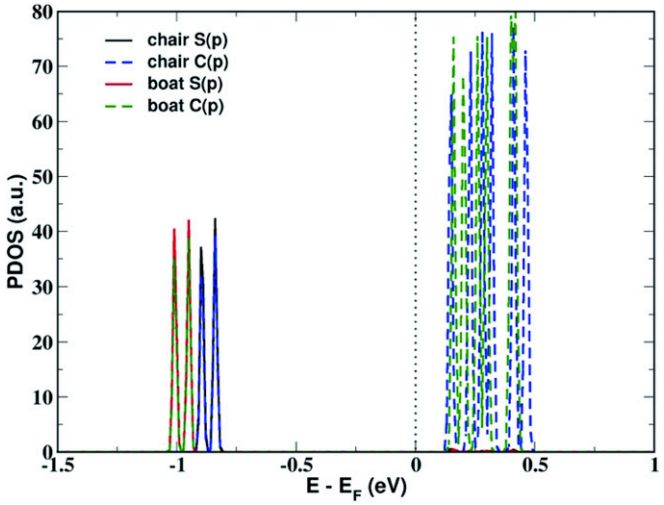

Fig. S3. PDOS of DBTTF-C_{60} in the boat and chair conformation as obtained from ground-state DFT calculations.

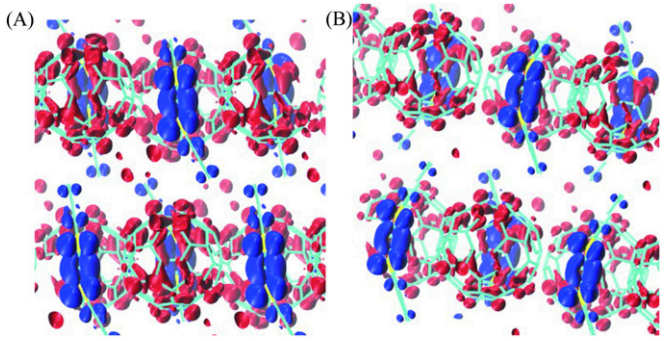

Fig. S4. Charge-density isosurfaces of the HOMO (blue) and LUMO (red) states for a DBTTF-C60 unit cell with DBTTF in the (*A*) chair- and (*B*) boat conformations.

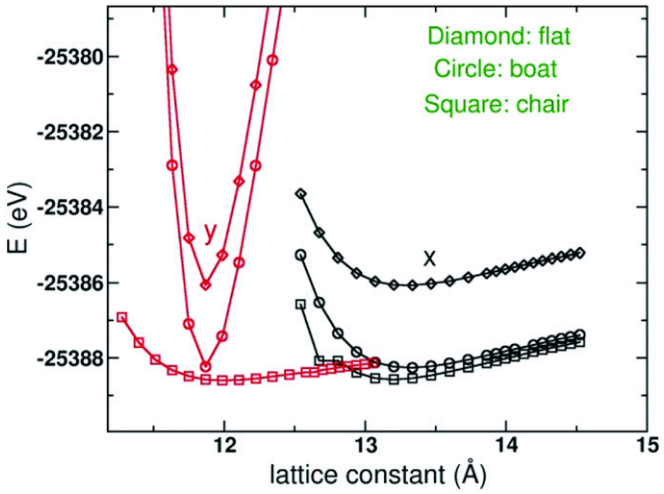

Fig. S5. Total energy as a function of lattice constant for a DBTTF-C60 unit cell in *x*- and *y* directions with DBTTF in the chair, boat, and flat (excited-state) conformations. The sharp curvature of the flat and boat conformation curves in the *y* direction is due to steric effects that are not present in the minimum energy chair conformation.

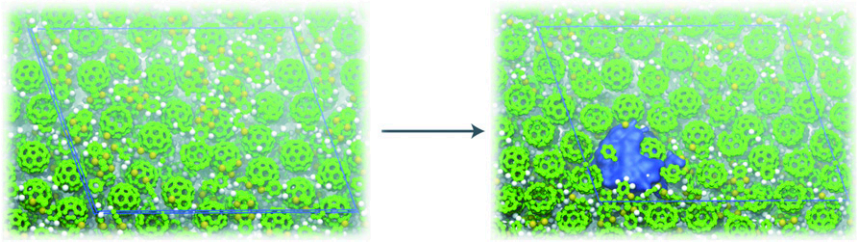

Fig. S6. Snapshots of the simulated bulk systems without (*Left*) and with (*Right*) an excess electron (blue). The pressure increases by roughly 2 kbar with the electron present. Blue lines indicate the periodically replicated simulation cell. Carbon, sulfur, and hydrogen atoms are colored green, yellow, and white, respectively.

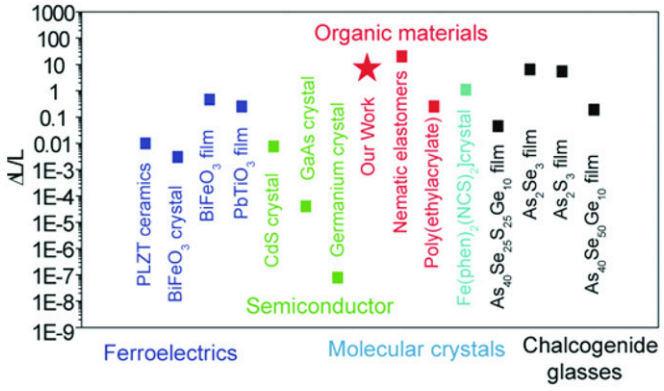

Fig. S7. Photostrictive properties in ferroelectrics, semiconductor, molecular crystals, chalcogenide glasses, and organic materials.

Table S1. HOMO (H), LUMO (L), and HOMO–LUMO (H-L) gap (electron volts) for a DBTTF-C60 unit cell with DBTTF in the chair and boat conformations

E, eV	Chair	Boat
H	−0.84	−0.95
L	0.15	0.16
H-L gap	0.99	1.11
Difference	0.12	—